Modeling of static development and dynamic behavior of the Electrical Double Layer at oil-pressboard interface

Juan M. Cabaleiro, Thierry Paillat, Olivier Moreau
and Gérard Touchard, *Member, IEEE*

***Abstract*— In this paper we model, as a first step, the formation of an electrical double layer (EDL) at a pressboard-oil interface without oil forced convection (static case). Then, once equilibrium is reached, convection is forced and EDL's dynamic behavior is studied. In this model, dissociation of a generic oil impurity into positive and negative ions is considered. Ion adsorption onto pressboard free sites, and desorption from occupied ones is allowed. Pressboard is considered permeable to a certain degree. Conservation of charged and neutral oil species, as well as evolution of occupied positive and negative pressboard sites, and solution of Navier-Stokes equations with Coulomb force term included are studied with a finite volume code developed by "Electricité de France" (i.e. Code Saturne). Finally, the results of dynamic behavior at different flow rates are compared to experimental results.**

***Index Terms*—Electrical Double Layer, dielectric liquid, short term transient.**

I. INTRODUCTION

MOST solid surfaces acquire a surface electric charge when brought into contact with an electrolyte (liquid). Mechanisms for the spontaneous charging of surface layers include the differential adsorption of ions from an electrolyte onto the solid surfaces, the differential solution of ions from the surface to the electrolyte, the deprotonation/ionization of surface groups [1], corrosion [2], or a combination of adsorption and corrosion [3]. These phenomena lead to the formation in the liquid of an Electrical Double Layer (EDL), formed by a "compact layer" and a "diffuse layer" according to the Stern model [4]. The compact layer is located between the solid wall and the maximum approach plan (passing by the center of ions attached to the wall). The diffuse layer is located between the maximum approach plan and the bulk of the liquid. The characteristic length of the diffuse part of the EDL is given by the Debye length. Charges present in the diffuse part of the double layer are convected when the liquid is made to flow. The convection of these charges gives rise to the phenomenon called "flow electrification". Although this phenomenon has been identified over a century ago, it is not yet completely understood. Different theoretical models have been proposed in the past, however, due to the strong coupling of the governing equations, most authors have made a number of hypotheses to simplify the problem to be solved. In general, the simplifying hypotheses concern the distribution of space charge, the physico-chemical interfacial processus responsible for the charging, or the problem dynamics.

Furthermore, very few [5] have addressed the transient existing at the beginning of the flow.

In this work we present a model for the formation of the EDL, and for the flow electrification phenomenon, analyzing particularly the initial transient. It is not the aim of this work to present a parametric study, but to present the model itself, and the numerical tools used to solve the equations system associated to it.

Manuscript received April 17, 2009. This work was supported in part by…….

J. M. Cabaleiro is with the CONICET, Laboratorio de Fluidodinámica, Departamento de Ingeniería Mecánica de la Facultad de Ingeniería de la Universidad de Buenos Aires. Av. Paseo Colón 850, Buenos Aires, Argentina. (corresponding author, phone: +5411-43430891 ext. 383; e-mail: jmcabaleiro@fi.uba.ar).

T. Paillat and G. Touchard are with the Laboratoire d'Etudes Aérodynamiques, UMR 6609 CNRS, Groupe Electrofluidodynamique, Université de Poitiers, 86962 Futuroscope Chasseneuil, France.

O. Moreau is with EDF R&D, 1 Avenue du Général de Gaulle, 92141 Clamart, France.

II. MODEL

A. Physico-chemical approach

Coming from research done for or by the petroleum industry, one generally accepted hypothesis is that space charge in the diffuse layer comes from preferential adsorption of ions that are present in low concentration, and in chemical equilibrium in the liquid [6]. We will apply this hypothesis to our case, where oil flows through a pressboard duct.

B. Problem's general equations

Most of the work done on this subject concerns the flow of dielectric liquids in metallic ducts [7]-[9]. On major difference between those cases and ours is that in this study the duct's walls are made of a porous, isolating material (pressboard). Therefore, we assume that physico-chemical reactions can also occur inside the pressboard region (penetrated by the oil). This leads to the formation of an EDL not only in the liquid region but in the pressboard as well (Fig. 1).

We also consider that the external side of the pressboard is in contact with an equipotential region (metallic electrode).

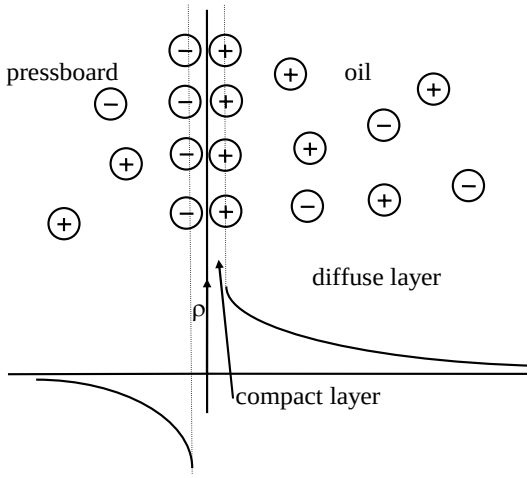

Fig. 1. Electrical double layer's scheme.

Pressboard behaves as a non moving fluid where chemical species react, diffuse and migrate (and are convected with a very low velocity) with rates that are different to those in the oil region.

Let us consider that only one kind of impurity is present in the oil. This neutral molecule can dissociate into positive and negative ions as follows:

$$A_L B_L \underset{K_{r1}}{\overset{K_{d1}}{\rightleftharpoons}} A_L^{+} + B_L^{-} \tag{1}$$

Then, flux densities of the three species are, in the oil region (medium 1):

$$\begin{aligned}
\overrightarrow{\Gamma_P} &= -D_P^1 \vec{\nabla} n_P - n_P \frac{e_0 . z_P . D_P^1}{kT} \vec{\nabla}\varphi + n_P . \vec{u} \\
\overrightarrow{\Gamma_N} &= -D_N^1 \vec{\nabla} n_N + n_N \frac{e_0 . z_N . D_N^1}{kT} \vec{\nabla}\varphi + n_N . \vec{u} \\
\overrightarrow{\Gamma_{neut}} &= -D_{neut}^1 \vec{\nabla} n_{neut} + n_{neut} . \vec{u}
\end{aligned} \tag{2}$$

and in the pressboard region (medium 2):

$$\begin{aligned}
\overrightarrow{\Gamma_P} &= -D_P^2 \vec{\nabla} n_P - n_P \frac{e_0 . z_P . D_P^2}{kT} \vec{\nabla}\varphi \\
\overrightarrow{\Gamma_N} &= -D_N^2 \vec{\nabla} n_N + n_N \frac{e_0 . z_N . D_N^2}{kT} \vec{\nabla}\varphi \\
\overrightarrow{\Gamma_{neut}} &= -D_{neut}^2 \vec{\nabla} n_{neut}
\end{aligned} \tag{3}$$

Where:

$\overrightarrow{\Gamma_{P,N}}$	ionic flux density vector ($m^{-2}s^{-1}$)
$\overrightarrow{\Gamma_{neut}}$	neutral flux density vector ($m^{-2}.s^{-1}$)
$D^i_{P/N/neut}$	positive, negative or neutral Diffusion coefficient in medium *i* ($m^2.s^{-1}$)
$n_{P/N/neut}$	positive, negative or neutral species number concentration (m^{-3})
e_0	elementary charge (1.6022 x 10^{-19} C)
$z_{P/N}$	positive/negative ions valence, taken as 1 in (1)
k	Boltzmann's constant (1.38 x 10^{-23} J/K)
T	absolute temperature (K)
φ	electric potential (V)
$\vec{u}$	velocity vector ($m.s^{-1}$)

As stated previously, it seems valid to assume chemical reactions between oil species and pressboard constituents within the whole pressboard region, rather than only at the interface (as it would be in the case of non-porous walls).

We model oil-pressboard interaction by the following generic chemical reactions:

$$\begin{aligned}
RN + B_L^{-} &\underset{K_{rN}}{\overset{K_{fN}}{\rightleftharpoons}} RB_L^{-} \\
RP + A_L^{+} &\underset{K_{rP}}{\overset{K_{fP}}{\rightleftharpoons}} RA_L^{+}
\end{aligned} \tag{4}$$

RN, RP	free active cellulose radicals
RB_L^-, RA_L^+	occupied cellulose radicals

Conservation equations of each species are, within the oil region:

$$\begin{aligned}
\frac{\partial n_P}{\partial t} + \vec{\nabla}\cdot\overrightarrow{\Gamma_P} &= K_{d1} n_{neut}^{\gamma} - K_{r1} n_P n_N \\
\frac{\partial n_N}{\partial t} + \vec{\nabla}\cdot\overrightarrow{\Gamma_N} &= K_{d1} n_{neut}^{\gamma} - K_{r1} n_P n_N \\
\frac{\partial n_{neut}}{\partial t} + \vec{\nabla}\cdot\overrightarrow{\Gamma_{neut}} &= -\gamma\left[K_{d1} n_{neut}^{\gamma} - K_{r1} n_P n_N\right]
\end{aligned} \tag{5}$$

and within the pressboard region:

$$\begin{aligned}
\frac{\partial n_P}{\partial t} + \vec{\nabla}\cdot\overrightarrow{\Gamma_P} &= K_{d2} n_{neut}^{\gamma} - K_{r2} n_P n_N + K_{rP} n_{RA^+} - K_{fP} n_P n_{RP} \\
\frac{\partial n_N}{\partial t} + \vec{\nabla}\cdot\overrightarrow{\Gamma_N} &= K_{d2} n_{neut}^{\gamma} - K_{r2} n_P n_N + K_{rN} n_{RB^-} - K_{fN} n_N n_{RN} \\
\frac{\partial n_{neut}}{\partial t} + \vec{\nabla}\cdot\overrightarrow{\Gamma_{neut}} &= -\gamma\left[K_{d2} n_{neut}^{\gamma} - K_{r2} n_P n_N\right] \\
\frac{\partial n_{RA^+}}{\partial t} &= -K_{rP} n_{RA^+} + K_{fP} n_P n_{RP} \quad with \quad n_{RA^+} + n_{RP} = N_P \\
\frac{\partial n_{RB^-}}{\partial t} &= -K_{rN} n_{RB^-} + K_{fN} n_N n_{RN} \quad with \quad n_{RB^-} + n_{RN} = N_N
\end{aligned} \tag{6}$$

With:

K_{di}	dissociation rate in medium *i* of reaction (1) (s^{-1})
K_{ri}	recombination rate in medium *i* of reaction (1) ($m^3.s^{-1}$)
$K_{fP/N}$	positive or negative ions adsorption rate ($m^3.s^{-1}$)
$K_{rP/N}$	positive or negative ions desorption rate (s^{-1})
n_{RA^+/RB^-}	number concentration of occupied sites by positive or negative ions ($1/m^3$)
$n_{RP/RN}$	number concentration of free sites that can react with positive or negative ions ($1/m^3$)
N_P, N_M	number concentration of active cellulose radicals ($1/m^3$)

One can then write Poisson's equation, in the liquid:

$$\vec{\nabla}\cdot\left(\varepsilon_1 \vec{\nabla}\varphi\right) = -e_0\left(z_p n_P - z_N n_N\right) \tag{7}$$

and in the pressboard:

$$\vec{\nabla}\cdot\left(\varepsilon_2 \vec{\nabla}\varphi\right) = -e_0\left(z_p n_P - z_N n_N + z_p n_{RA^+} - z_N n_{RB^-}\right) \tag{8}$$

where ε_i is the dielectric permittivity of medium *i*.

Finally, in medium 1 (the oil region), due to convective transport of the species present, the previous equations are coupled to Navier-Stokes equations (incompressible, Newtonian fluid of constant viscosity):

$$\rho_m \frac{D\vec{u}}{Dt} = -\vec{\nabla}P + \rho_m \vec{\mathbf{g}} + \mu\Delta\vec{u} - e_0\left(z_p n_P - z_N n_N\right)\vec{\nabla}\varphi \tag{9}$$

In (9), ρ_m is the mass density, P is the pressure and μ the dynamic viscosity.

In the porous region, we have added a source term to the NS equations:

$$\rho_m \frac{D\vec{u}}{Dt} = -\vec{\nabla}P + \rho_m \vec{\mathbf{g}} + \mu\Delta\vec{u} - e_0\left(z_p n_P - z_N n_N\right)\vec{\nabla}\varphi - \frac{\mu}{\kappa}\vec{u} \quad (10)$$

As the term μ/κ is very important, solving (10) is analogous to solving the Darcy equation inside the pressboard:

$$\overrightarrow{U_{carton}} = -\frac{\kappa}{\mu}\vec{\nabla}P \quad (11)$$

with an agreement zone between both flows.

The previous equations system has been implanted in Code-Saturne, a code developed by Electricité de France (EDF) for the resolution of Navier-Stokes equations with the finite volumes method. Dedicated modules are available for specific physics such as radiative heat transfer, combustion (gas, coal, heavy fuel oil, …), magneto-hydrodynamics, etc. [10]. We have developed a module called ionic conduction which couples and solves the system (5)-(10).

Simulation is undertaken in two phases:

1) Static development of the EDL: starting from uniform initial concentrations of all species, adsorption/desorption reactions are allowed to start, and simulation is continued until the electrical current through the interface becomes negligible.

2) Once static equilibrium is reached, a Poiseuille flow is imposed at the entry and the effect of convection is studied.

First results obtained with this model, where calculated as if only one of the ionic species reacted with cellulose, the negative ions B_L^-. Values of the physical constants of both mediums and of ionic species are presented in table 1.

TABLE I
PHYSICAL CONSTANTS.

Constant	Symbol	Value
Oil permittivity	ε_h	$2.2\varepsilon_0$
Pressboard permittivity	ε_c	$4\varepsilon_0$
Dynamic viscosity	η	0.0146 kg/(m.s)
Oil mass density	ρ_{mh}	836.9 kg/m^3
Pressboard mass density	ρ_{mc}	1190 kg/m^3
Positive ions mobility in oil	μ_P	10^{-9} m^2/(V.s)
Negative ions mobility in oil	μ_N	10^{-9} m^2/(V.s)
Ions valence	Z	1
Ions charge	q=Ze	$1.6\ 10^{-19}$ C
Positive ions diffusion coefficient in oil	$D_P=\mu_P\ kT/\|q\|$	$2.5\ 10^{-11}$ m^2/s
Negative ions diffusion coefficient in oil	$D_N=\mu_N\ kT/\|q\|$	$2.5\ 10^{-11}$ m^2/s

C. Reaction rates and initial concentration values:

The recombination coefficient is related to the medium's permittivity and to ions mobility by the Langevin relation [11]:

$$K_{ri} = \frac{e_0}{\varepsilon_i}\left(\mu_P^i + \mu_N^i\right) \quad (12)$$

Let n_0 be the initial number concentration of positive and negative ions (as charge density is zero throughout the entire volume at the beginning of the simulation, positive and negative ion concentrations must be equal). Assuming chemical species to be in equilibrium we have:

$$K_{di}.{n_{neutr0}}^{\gamma} = K_{ri}.{n_0}^2 \quad (13)$$

combining (12) and (13), we obtain:

$$K_{di} = \frac{e_0}{\varepsilon_i}\left(\mu_P^i + \mu_N^i\right)\frac{n_0^2}{{n_{neutr0}}^{\gamma}} \quad (14)$$

Defining an ionization factor p:

$$p = \frac{n_0}{n_{neutr0}} \quad (15)$$

related to the ionized fraction θ by:

$$p = \frac{\theta}{1-\theta} \quad (16)$$

we can write:

$$K_{di} = \frac{e_0}{\varepsilon_i}\left(\mu_P^i + \mu_N^i\right)n_0^{2-\gamma}\,p^{\gamma} \quad (17)$$

An order of magnitude of n_0 can be obtained from the medium's bulk conductivity:

$$\sigma_{0i} = e_0 n_0\left(\mu_P^i + \mu_N^i\right) \quad (18)$$

The measured bulk conductivity is $0.5\text{x}10^{-12}$ S/m for the oil and $0.5\text{x}10^{-13}$ S/m for our oil impregnated pressboard. We assume that the difference in conductivity is due to a difference in ions mobility, and therefore the initial number concentrations of the chemical species are equal in both mediums.

For an ionized fraction $\theta = 0.1$ (which is quite high), and a reaction order $\gamma = 1$, the following values were obtained:

TABLE II
INITIAL VALUES AND REACTION RATES.

Parameter	Symbol	Value
Initial ions concentration in oil	n_{01}	$1.56\ 10^{15}$ ions/m^3
Initial neutral molecule concentration in oil	$n_{neutr01}$	$1.4\ 10^{16}$ molec./m3
Initial ions concentration in pressboard	n_{02}	$1.56\ 10^{15}$ ions/m3
Initial neutral molecule concentration in pressboard	$n_{neutr02}$	$1.4\ 10^{16}$ molec./m^3
Recombination rate in oil	K_{r1}	$1.65\ 10^{-17}$ m^3.s^{-1}
Dissociation rate in oil	K_{d1}	$2.85\ 10^{-3}$ s^{-1}
Recombination rate in pressboard	K_{r2}	$9.05\ 10^{-19}$ m^3.s^{-1}
Dissociation rate in pressboard	K_{d2}	$1.57\ 10^{-4}$ s^{-1}

The number concentration of active cellulose radicals (N_P and N_N) are not easy to determine. Bourgeois [12] states that the total number of carboxyl groups (RCOOH) contained in pressboard is $11x10^{-3}$ mol/100 gr. That is, a number concentration of $7.88x10^{25}$ m^{-3}. The availability of these groups seems indispensable for oil-cellulose reactions to take place. However, the number of sites likely to react could be quite smaller [12]. Nevertheless we have assumed as an order of magnitude that $N_P=N_N= 10^{25}$ sites/m^3.

In previous work [13]-[14] we have presented macroscopic models of flow electrification where a wall current density responds to the following equation:

$$i_w = K[\rho_{w\infty} - \rho_w] \quad (19)$$

where K is a global adsorption rate, and ρ_w and $\rho_{w\infty}$ are the charge density near the wall and that of a fully developed EDL.

Matching that model with experimental results gave a value for of $K=2x10^{-6}$ $m.s^{-1}$.

Furthermore, considering that reactions occur in a certain representative volume (*vol*), limited by an interface of surface *A*, *K* can be estimated with the following expression [15]:

$$K = \frac{vol}{A}\frac{K_{fN}.n_{N0}}{2.(n_{N0}-n_{Neq})}n_{RN} \quad (20)$$

Assuming that equilibrium concentration of negative ions is negligible, the adsorption rate of negative ions is:

$$K_{fN} \approx \frac{A}{vol}\frac{2K}{n_{RN}} \quad (21)$$

For a ratio A/vol on the order of $1/\delta_0$ we get $K_{fN} = 1.28x10^{-26}$ $m^3.s^{-1}$.

At equilibrium we must have:

$$K_{rN} n_{RB^-eq} = K_{fN} n_{Neq} n_{RNeq} \quad (22)$$

As the number concentration of active cellulose radicals is enormous compared to the number concentration of negative ions, at equilibrium the number concentration of unoccupied negative sites is practically the initial concentration:

$$n_{RNeq} \approx N_N \quad (23)$$

Therefore the desorption rate is:

$$K_{rN} = K_{fN} N_N \frac{n_{Neq}}{n_{RB^-eq}} \quad (24)$$

This rate is a function of the ratio of negative ions to occupied negative sites concentrations at equilibrium. This ratio is unknown “a priori”. Several values have been tested and have to be adjusted. We present here results with K_{rN} = 1.28 10^{-3} s^{-1} (which is a high desorption rate corresponding to a ratio of 0.01).

D. Geometry, mesh and boundary conditions

The geometry used for the simulation is based upon the facility used to obtain the experimental results [16]. It consists of a rectangular pressboard duct where oil is forced to flow in a laminar regime. The outer side of the pressboard duct is in contact with grounded metallic surfaces (Fig. 2).

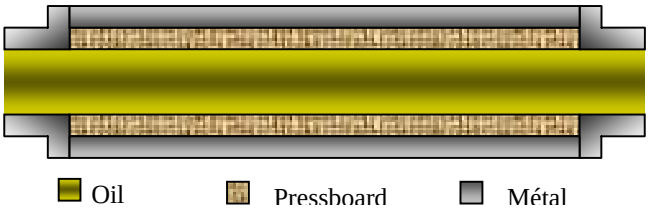

Fig. 2. Scheme of the pressboard duct, surrounded by metallic electrodes and couplings.

The mesh used represents half of the duct (3 mm between plates, 30 mm wide and 100 mm long; pressboard width: 1.5 mm), and we analyze the problem as if it were bi-dimensional (flow between two plates). This has been done to reduce the number of cells (Fig 3), which is 19000: 100x1x100 in the upper side, and 100x1x90 in the lower side). The characteristic length of the EDL, δ_0, is considerably smaller than the duct’s half height. For that reason, the mesh has been refined near the interface, where the gradients are stronger.

Cell’s characteristic sizes in the *X* direction are:

ΔX_{min}=4 x 10^{-9} m

ΔX_{max}=1.5 x 10^{-4} m

These cell sizes allow for 64 cells to fit in a distance δ_0 from the wall, and 75 cells in a distance of $3\delta_0$.

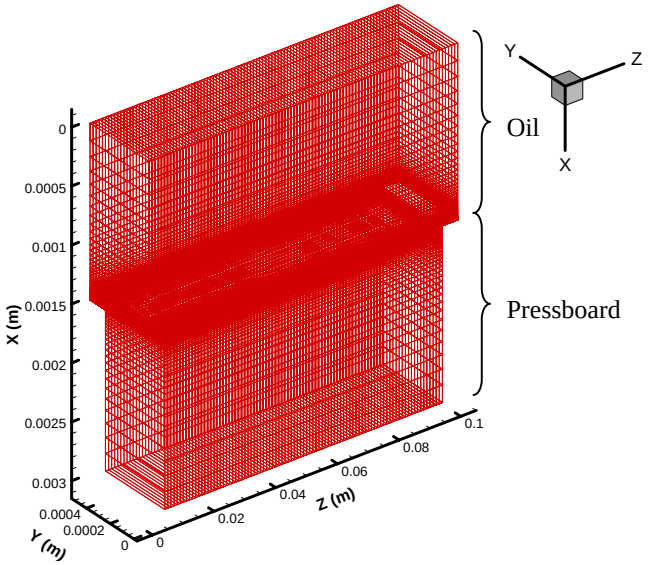

Fig. 3. Mesh and coordinate system.

Boundary conditions used for the simulation were (Fig. 4):

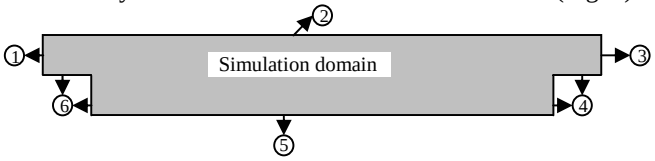

Fig. 4. Boundary conditions.

On the surfaces number 4, 5 and 6: walls, electric potential is null.

On surface number 1: symmetry in static development, and entry (Poiseuille velocity profile for $u_z(X)$) in dynamic simulation.

On surface number 3: symmetry in static development, and exit in dynamic simulation.

On surface number 2 and on surfaces Y=0 and Y=0.0005: symmetry.

III. Results

Prior to this simulation, static development was studied in a reduced configuration to better understand the influence of adsorption and desorption rates, ionized fraction, etc. The results of this study are discussed in [15] and are not presented here. Nevertheless, the results of that study allowed determining the necessary number of time steps to reach static equilibrium, for instance.

With the constants and initial values presented previously, static equilibrium is simulated with a time step of 1s, for 12000 steps.

Then, a Poiseuille flow is imposed at the entry and the simulation is run for 2000 time steps of 0.01 s. This was done for several mean velocities (0.1, 0.2, 0.4 and 0.6 m.s^{-1}).

Fig. 5 shows the space charge at static equilibrium. Space charge is positive in the oil region, and negative in the pressboard region (as expected).

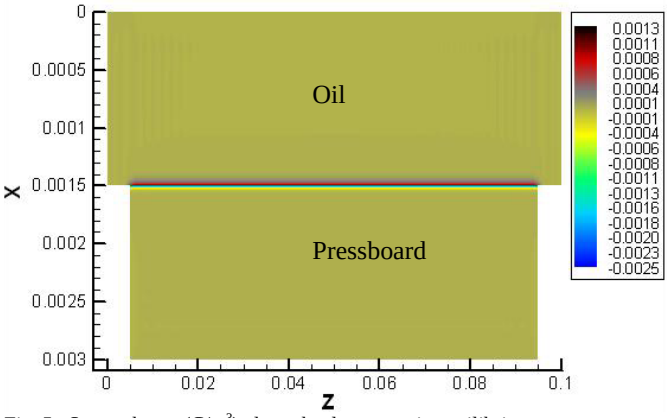

Fig. 5. Space charge (C/m^3) along the duct at static equilibrium.

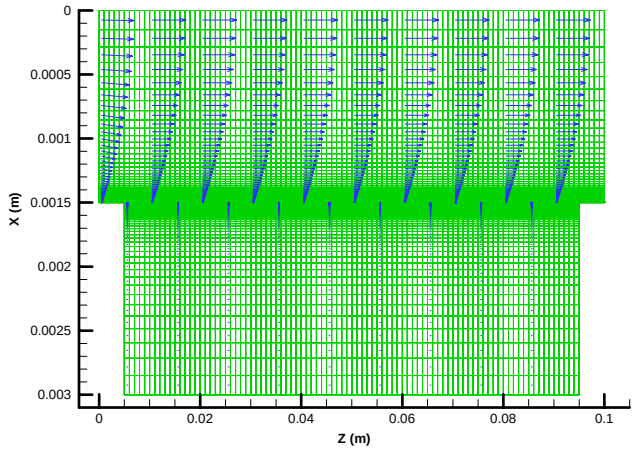

Fig. 6. Velocity field. Mean velocity: 0.1m.s^{-1}.

In order to use the Darcy source term on the Navier-Stokes equations, it is necessary to know the pressboard's permeability. Moreau [17] determined that these pressboards permeability is on the order of κ=10^{-16} m^2.

With this permeability, the velocity field obtained is (Fig. 6) practically the one of a Poiseuille flow.

The velocity profile near the interface is very important because it controls the dynamic formation of the EDL. Fig. 7 shows the evolution of space charge along the duct, during the first ten seconds of flow. The scale is reduced to have a closer look to the interface region. The space charge, which is homogenous along the duct at the beginning, is swept by the flow. It evolves towards a dynamic equilibrium regime where space charge increases progressively along the channel. Inside the pressboard, the space charge increases with time at every point, with a zone close to the entry where charge accumulation is more important.

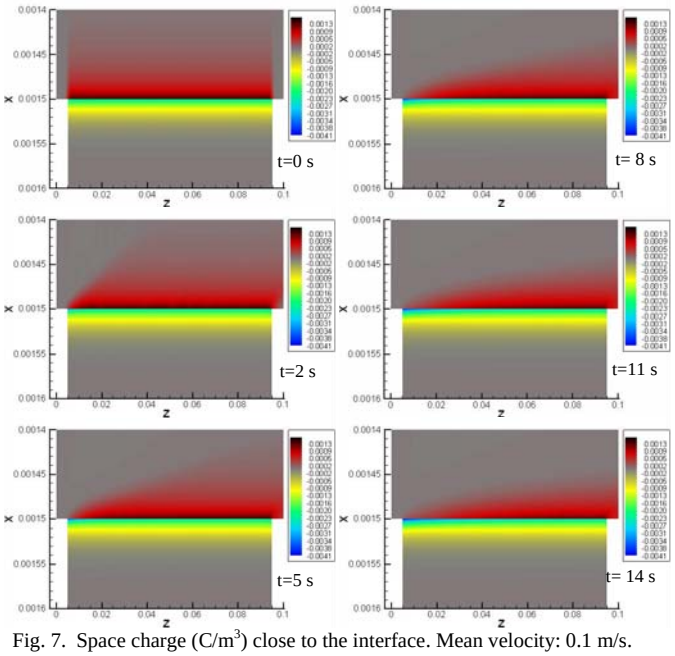

Fig. 7. Space charge (C/m^3) close to the interface. Mean velocity: 0.1 m/s.

Electric potential gives an idea of the location of charge accumulation regions: close to the interface and to the pressboard duct's entry (Fig 8).

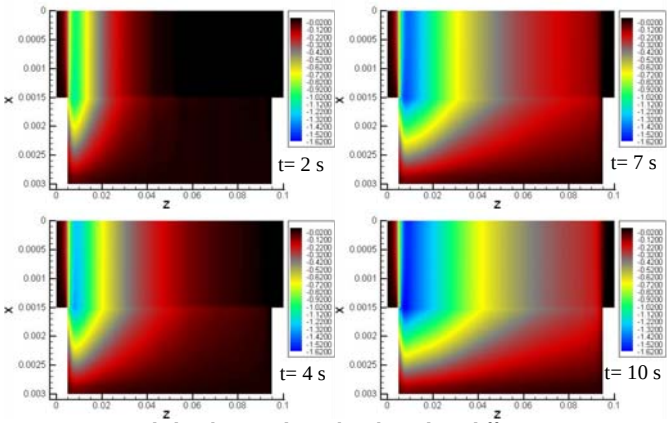

Fig. 8. Potential distribution along the channel at different times. Mean velocity: 0.1 m.s^{-1}.

In Fig. 9 and Fig. 10 we present the space charge and the electric potential plots, at the interface along the duct, in the liquid region (X=1.5 mm), for the four velocities simulated.

In Fig. 11 a plot is presented of the space charge profiles in the liquid region, at 9 different axial positions: 0.01m<Z<0.09m, at t=10s. In the same figure, a plot of the space charge profile at static equilibrium is presented for comparison. As the axial coordinate increases, the space charge near the wall seems to tend to the static (fully developed) value. However, charge distribution in the direction normal to the wall is more compact than the static EDL case, even for the lowest velocity simulated. This shows that the hypothesis of instantaneous distribution of charges in the direction normal to the wall, as compared to the residence time of a particle being convected, should be made with precaution in the case of oil flowing in a pressboard duct. The opposed hypothesis, that is, the instantaneous formation of all the space charge at the interface and then its diffusion is not applicable (for the reaction rates considered at least) because the integral of the space charge at constant Z increases along the duct.

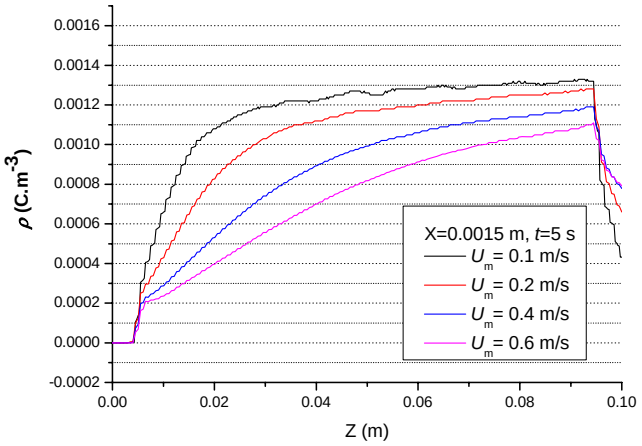

Fig. 9. Space charge at the interface, in the liquid. t=5s.

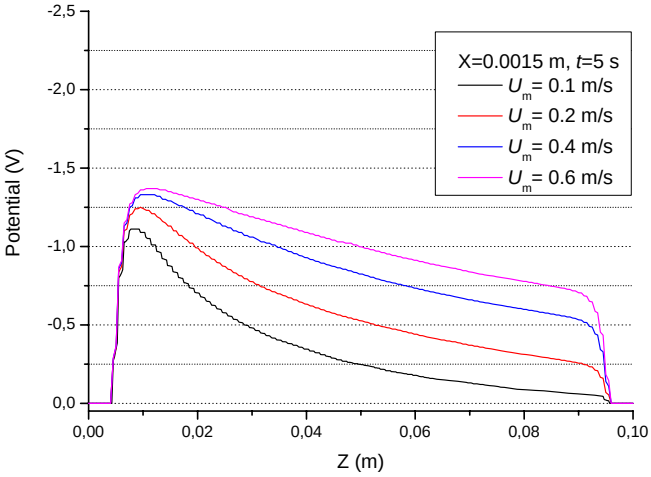

Fig. 10. Electric potential at the interface, in the liquid. t=5s.

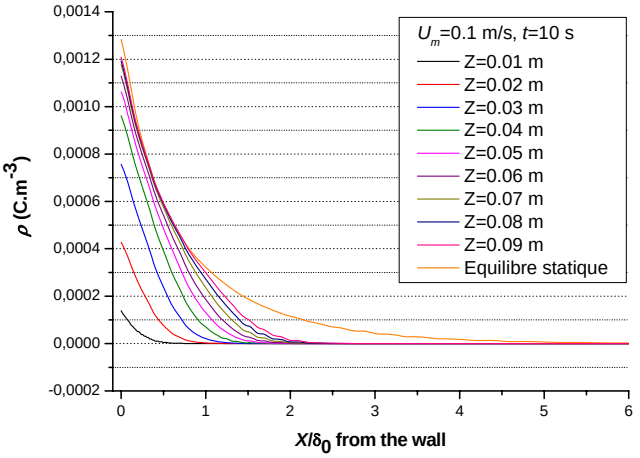

Fig. 11. Space charge profiles in the liquid along the duct. Mean velocity: 0.1 m/s, t=5s.

Finally, the current density has been integrated at the duct's exit to obtain the streaming current, in order to compare these results to those obtained in our experimental facility. Fig. 12 presents the streaming current as a function of time, for the four velocities studied.

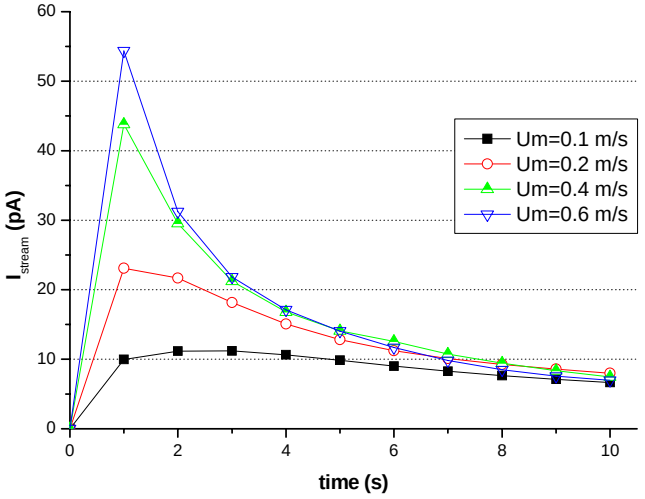

Fig. 12. Streaming current (numerical) as a function of time, for the four mean velocities studied.

Experimental results show that the streaming current's peak value is reached about 5s after the pump is started. In our simulation this maximum is reached faster than that. This is probably due to the fact that the velocity profile is imposed instantaneously in the simulation, but the pump takes a few seconds to attain its stationary regime. Also, the filtering produced by the pico-ammeters used contributes to retarding the signal. Nevertheless, experimental and numerical curves qualitatively resemble each other regarding the dynamic and the orders of magnitude.

We have to remark, however, that at t=5s approximately, streaming current for the highest velocity (0.6 m.s^{-1}) becomes smaller than a lower velocity (0.4 m.s^{-1}) streaming current. The same is observed at t=8s between the third (0.4 m.s^{-1}) and second (0.2 m.s^{-1}) velocity. This particular behavior has not been observed experimentally. In fact, we have always found

in our experiments that streaming current increases with the flow's mean velocity.

IV. Conclusion

We have presented a model for the formation of an Electrical Double Layer, without flow, and with a laminar flow in a rectangular duct. We used a generic adsorption/desorption reaction as the source for the formation of the EDL at the interface between a dielectric liquid and an isolating-porous material. The equations governing this problem are coupled and nonlinear which makes the interpretation of the results rather complicated. Nevertheless, some behaviors have been identified.

First, space charge distribution along the duct shows that, for the reaction rates used and for the relaxation time of the liquid considered, neither the instantaneous space charge profile establishment nor the instantaneous formation of all the space charge at the interface (and then its diffusion) seem applicable hypotheses. The solution is found to be in between those two asymptotic descriptions.

Second, although some issues need be further studied, the resemblance between experimental and numerical results concerning the streaming current is encouraging.

We believe that this model is particularly interesting, because it is not only useful for flow electrification problems, but for electroosmosis (inverse problem where the application of an electric field produces the flow) problems. This means that the model could be applied with some minor modifications to microfluidics problems.

References

[1] R. J. Hunter, *Zeta Potential in Colloid Science*, Academic Press, London, 1981.

[2] G. Touchard, T. W. Patzek. C.J. Radke, "A physicochemical explanation for flow electrification in low-conductivity liquids in contact with a corroding wall," *IEEE Trans. Ind. App*., vol. 32, No. 5, pp. 1051-1057, Sept. 1996.

[3] A. P. Washabaugh and M. Zhan, "A chemical reaction-based boundary condition for flow electrification," *IEEE Transactions on Dielectrics and Electrical Insulation*, vol. 4, No. 6, pp. 688–709, Dec. 1997.

[4] O. Stern, "Zur Theorie der Electrolytischen", Z. Elektrochem. Vol. 30, pp. 508-516. 1924.

[5] J. A. Palmer and J. K. Nelson, "The simulation of short-term streaming electrification dynamics," .*J. Phys. D: Appl. Phys.*, vol. 30, pp. 1207-1213, 1997.

[6] A. Klinkerberg, J.L. Van der Minne, *Electrostatics in Petroleum Industry*, Elsevier, Amsterdam, 1958.

[7] B. Abedian, "Electric Charging of Low Conductivity Liquids in Turbulent Flows through Pipes," PhD Thesis M.I.T. 1979.

[8] A. A. Boumans, "Streaming current in turbulent flows and metal capillaries," *Physica XXIII*, pp. 1007-1055, 1957.

[9] S. Andriamitanjo, "Electrisation d'un hydrocarbure s'écoulant dans un tube métallique en régime laminaire," Thesis of INP of Grenoble, 1981.

[10] "Code_Saturne : a Finite Volume Code for the Computation of Turbulent Incompressible Flows," *Industrial Applications, International Journal on Finite Volumes*, Vol. 1, 2004.

[11] R. Tobazéon, "Conduction électrique dans les liquids," *Techniques de l'Ingénieur*, D 2 430.

[12] A. Bourgeois, "Etude du phénomène d'électrisation par écoulement sur les cartons des transformateurs de puissance," Thesis of INP of Grenoble, 2007.

[13] J. M. Cabaleiro, T. Paillat. O. Moreau and G. Touchard, "Electrical double layer's development analysis: application to flow electrification in power transformers," *IEEE Trans. Ind. App*., vol. 45, No. 2, pp. 597-605, 2009.

[14] J. M. Cabaleiro, T. Paillat. O. Moreau and G. Touchard, "Flow electrification of dielectric liquids in insulating channels: Limits to the application of the classical wall current expression," *J. of Electrostatics*, vol. 66, pp. 79-83, 2008.

[15] J. M. Cabaleiro, "Etude du développement de la double couche électrique lors de la mise en écoulement d'un liquide diélectrique dans une conduite isolante," Thesis of the LEA of Poitiers, 2007.

[16] O.Moreau, T. Paillat, and G. Touchard, "Flow electrification in transformers: Sensor prototype for electrostatic hazard," Electrostatics, pp. 31–36, Mar. 2003.

[17] E. Moreau, T. Paillat et G. Touchard, "Flow electrification in high power transformers: BTA effect on pressboard degraded by electrical discharges," *IEEE Transactions on Dielectrics and Electrical Insulation*, Vol. 10, No. 1, pp. 15-21, 2003.